

Artificial Faraday rotation using a ring metamaterial structure without static magnetic field

Toshiro Kodera, Dimitrios L. Sounas, and Christophe Caloz

Citation: *Appl. Phys. Lett.* **99**, 031114 (2011); doi: 10.1063/1.3615688

View online: <http://dx.doi.org/10.1063/1.3615688>

View Table of Contents: <http://apl.aip.org/resource/1/APPLAB/v99/i3>

Published by the [AIP Publishing LLC](#).

Additional information on *Appl. Phys. Lett.*

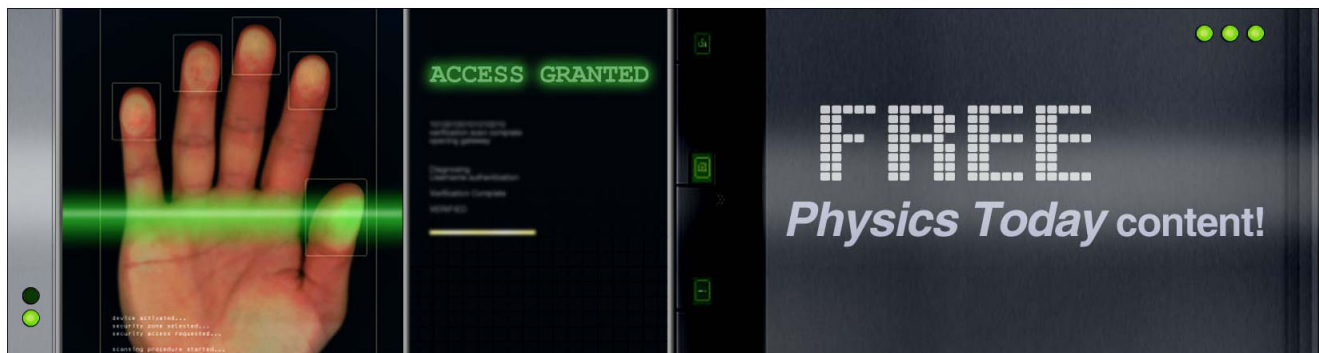
Journal Homepage: <http://apl.aip.org/>

Journal Information: http://apl.aip.org/about/about_the_journal

Top downloads: http://apl.aip.org/features/most_downloaded

Information for Authors: <http://apl.aip.org/authors>

ADVERTISEMENT



Artificial Faraday rotation using a ring metamaterial structure without static magnetic field

Toshiro Kodaera,^{1,a)} Dimitrios L. Sounas,^{2,b)} and Christophe Caloz^{2,c)}

¹Department of Electrical Engineering, Yamaguchi University, Ube 7558611, Japan

²Department of Electrical Engineering, École Polytechnique de Montréal, Montréal, Québec H3T 1J4, Canada

(Received 9 June 2011; accepted 1 July 2011; published online 20 July 2011)

A metamaterial structure composed of a periodic array of conductive rings including each a semiconductor-based isolator is experimentally shown to produce Faraday rotation. Due to the presence of the isolators, a unidirectional traveling-wave regime is established along the rings, generating rotating magnetic moments and hence emulating the phenomenon of electron spin precession. The metamaterial exhibits the same response as a magnetically biased ferrite or plasma, but without the need of any static magnetic field bias, and therefore, it is easily integrated in printed circuit technology. © 2011 American Institute of Physics. [doi:10.1063/1.3615688]

Faraday rotation, i.e., the non-reciprocal rotation of the polarization of an electromagnetic wave as it propagates through a medium, is the governing phenomenon of non-reciprocal devices such as isolators and circulators from microwave to optical frequencies.¹ Two different types of media are known to exhibit Faraday rotation: ferrites at microwave and optical frequencies and plasma semiconductors at optical frequencies.^{1,2} Both provide Faraday rotation when biased by a static magnetic field, usually produced by permanent magnets or electromagnets, and therefore, they are difficult to integrate in printed circuit technology.

Here, we propose an artificial material, or metamaterial,^{3,4} which provides Faraday rotation without static magnetic field bias. The metamaterial consists of a periodic arrangement of conductive rings loaded with unidirectional semiconductor components and it is fully integrable in printed circuit technology. The bias condition required for non-reciprocity is achieved through a static voltage which biases the unidirectional component. The proposed metamaterial behaves similarly to a ferrite.

In ferrite, Faraday rotation is the result of electron spin precession around the bias magnetic field, as illustrated in Fig. 1(a). This precession creates a rotating magnetic moment perpendicular to the bias magnetic field, which interacts differently with right-handed and left-handed circularly polarized (CP) waves, resulting in different refractive indices for the two types of CP waves. Consequently, the polarization of an elliptically polarized wave (or of a linearly polarized wave in the limiting case of an ellipse with zero ellipticity) propagating in the ferrite medium parallel to the bias magnetic field undergoes progressive rotation with an angle that is proportional to the difference of these refractive indices. Similarly, each ring of the proposed structure provides a rotating magnetic moment, as illustrated in Fig. 1(b). Specifically, each ring is loaded with a semiconductor-based isolator, which allows propagation only in one direction.

Therefore, a traveling wave propagates along the ring, producing a rotating magnetic field and, hence, a rotating magnetic moment, parallel to the plane of the ring.

The generation of the rotating magnetic moment in the proposed ring is further explained in Fig. 2 for the case of an ideal isolator with zero insertion loss, infinite isolation and zero-phase-shift transmission. Such a ring exhibits a traveling-wave resonance when its circumference is equal to the guided wavelength in the ring. Figure 2(a) depicts the time-dependent azimuthal θ -directed current in the ring at quarter-period spaced instants. Additionally, an azimuthal current flows in the opposite direction on the ground below the ring. The two currents create a radial magnetic field in the dielectric substrate between the ring and the ground, as shown in Fig. 2(b). This magnetic field can be assimilated to a radial magnetic moment rotating around the ring axis with an angular velocity equal to the radian resonance frequency of the ring.

Figure 3 shows a practical implementation of the proposed metamaterial, which consists of super-cells with four isolator-loaded rings each in a 90° rotational symmetry configuration and a double-layer dielectric with a conductive ground plane separation. The RF part of the cell, which includes the rings and the isolators, is placed on the front side—the side that will be illuminated by an incident wave—as shown in Fig. 3(b). The isolators are realized by common-source field effect transistors connected to the ring

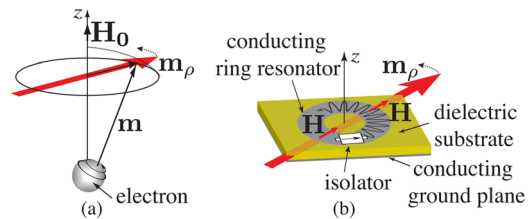


FIG. 1. (Color online) Rotating magnetic moment in (a) a ferrite, as a result of the electron spin precession around the bias magnetic field, and (b) in the proposed metamaterial structure, as a result of a traveling wave propagating along the ring. The ring is loaded with a semiconductor-based isolator in order to produce a traveling-wave regime.

^{a)}Electronic mail: tk@yamaguchi-u.ac.jp.

^{b)}Electronic mail: dimitrios.sounas@polymtl.ca.

^{c)}Electronic mail: christophe.caloz@polymtl.ca.

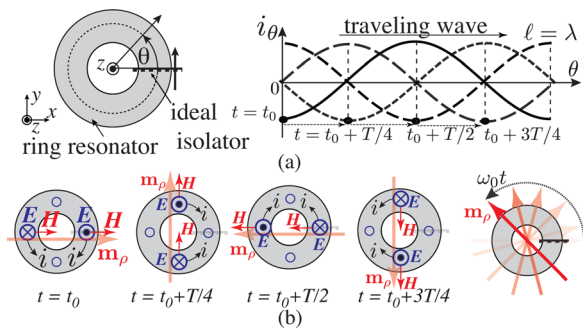


FIG. 2. (Color online) Conductive ring loaded with an ideal isolator. The ring resonates when its circumference equals the guided wavelength. (a) Ring geometry and azimuthal current along the ring at four quarter-period spaced time instants. (b) Magnetic field between the ring and the ground plane and corresponding effective magnetic moment at the time instants of Fig. 2(a).

via two by-pass capacitors of 1 pF. Moreover, two resistors, of 68 Ω and 100 Ω, are connected to the ground from the gate and the drain, respectively, for matching. The transistor biasing network, depicted in Fig. 3(c), is placed on the back side, so as to avoid any possible interference with the wave incident on the structure. It comprises a series inductor (meander line) and a shunt capacitor of 1000 pF, acting together as a low-pass filter to prevent the RF current from leaking into the DC voltage source. Fig. 4 shows an experimental prototype of the overall metamaterial consisting of 3 × 3 super-cells.

Due to the presence of the ground plane, which is only perforated by largely sub-wavelength holes for connection to the biasing network on the back dielectric layer, the structure of Figs. 3 and 4 is opaque to electromagnetic waves. Conse-

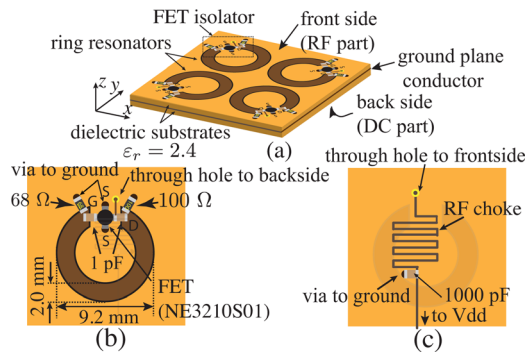


FIG. 3. (Color online) Practical implementation of the proposed metamaterial. The bias voltage to the FET isolator is provided through via from the back side to the front side, penetrating the ground conductor. (a) Unit-cell consisting of 4 rings in a 90° symmetry. (b) RF part on the front side. (c) DC biasing network on the back side.

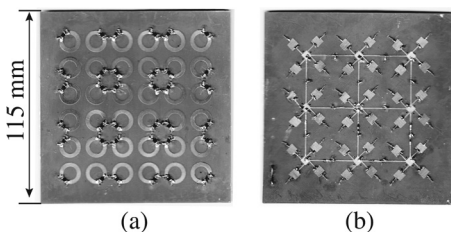


FIG. 4. Prototype of the proposed metamaterial, consisting of 9 (3 × 3) unit cells. (a) Front side. (b) Back side.

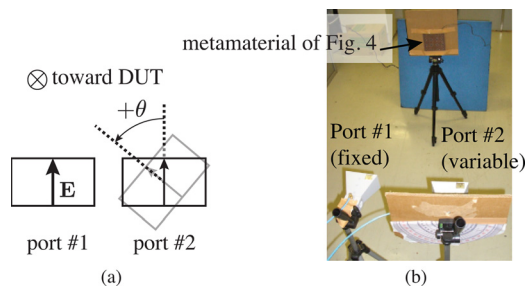


FIG. 5. (Color online) Measurement setup. (a) Two horn antennas, one with fixed polarization and the other one with variable polarization. (b) Whole setup showing the two horn antennas and the structure.

quently, Faraday rotation will manifest itself here in terms of rotation of the polarization of the wave reflected by the structure, a phenomenon known as the magneto-optical Kerr effect in bulk materials.² The corresponding measurement setup consists of two horn antennas pointing towards the structure, as shown in Fig. 5. One of the antennas has fixed polarization, while the other antenna is polarized at a variable relative angle θ with respect to the first one. The distance between the antennas and the structure is 1.5 m (37.5 wavelengths at 7.5 GHz) for far-field (plane wave) condition. These antennas are connected to a vector network analyzer, and time gating is applied to eliminate any direct coupling.

A simplified representation of the two-antenna setup for excitation from both ports is shown in Fig. 6, which also represents the reflected fields, assuming linear polarization and rotation of an angle $\varphi(\omega)$. The signal received by port 2 for excitation by port 1 is the projection of the reflected field on port 2, or in mathematical formalism,

$$S_{21}(\omega, \theta) = R(\omega)\cos[\theta - \varphi(\omega)], \tag{1}$$

where $R(\omega)$ is the reflected field magnitude, whereas the signal received by port 1 for excitation by port 2 is

$$S_{12}(\omega, \theta) = R(\omega)\cos[\theta + \varphi(\omega)]. \tag{2}$$

Equation (1) indicates that, for fixed θ , $|S_{21}|$ must be minimum at the frequency ω_{21}^{\min} where $\cos[\theta - \varphi(\omega_{21}^{\min})] = 0$ or $\varphi(\omega_{21}^{\min}) = \theta \pm \pi/2$, while Eq. (2) indicates that $|S_{12}|$ must be minimum at the frequency ω_{21}^{\min} where $\varphi(\omega_{21}^{\min}) = -\theta \pm \pi/2$. Therefore, an explicit relation between φ and ω follows from identification of the frequencies ω_{21}^{\min} and ω_{21}^{\min} for any $\theta \in [-\pi/2, \pi/2]$. Notice that an analogous extraction procedure from the maxima of $\cos[\theta \pm \varphi(\omega)]$ is not valid, since these do not necessarily coincide with the maxima of $|S_{21}|$ and $|S_{12}|$ due to $R(\omega)$.

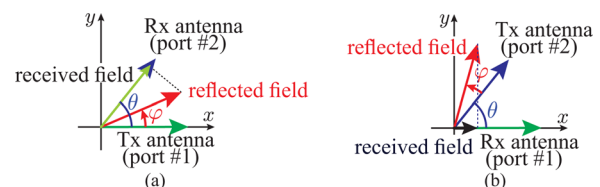


FIG. 6. (Color online) Simplified representation of the two-antennas setup with reflected and received fields. (a) Excitation at port 1. (b) Excitation at port 2.

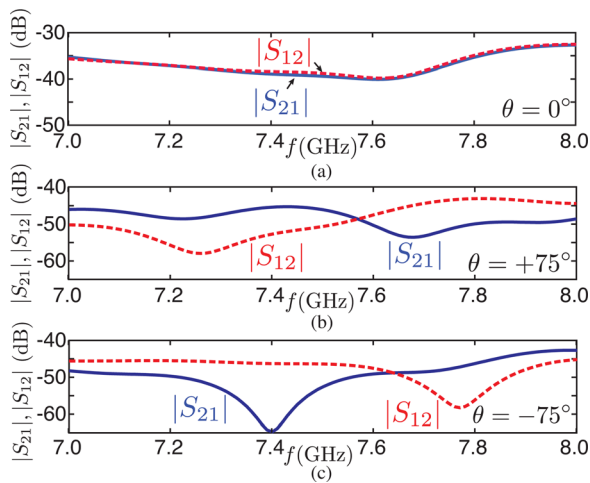


FIG. 7. (Color online) Measured transmission parameters between the two horns for different θ and $V_{DS}=0.57$ V. (a) $\theta=0^\circ$. (b) $\theta=+75^\circ$. (c) $\theta=-75^\circ$.

Figure 7 plots the magnitude of the measured S-parameters for a bias voltage $V_{DS}=0.57$ V (maximum voltage before instability) and several values of θ . For $\theta=0^\circ$ [Fig. 7(a)], $|S_{21}| \approx |S_{12}|$, as expected from Eqs. (1) and (2). In contrast, for $\theta=75^\circ$ [Fig. 7(b)], $|S_{21}|$ and $|S_{12}|$ are completely different, a fact also predicted by the different arguments of the cosines in Eqs. (1) and (2). Moreover, if the sign of θ is reversed [Fig. 7(c)], the responses of $|S_{21}|$ and $|S_{12}|$ are reversed as well. The minima are clearly observed, thereby allowing an accurate extraction of φ following the procedure described in the previous paragraph.

Figure 8(a) presents the polarization rotation angle φ versus frequency, as extracted from measured S-parameters. As expected, the observed frequency dependence of the rotation angle, with direction reversal at the resonance, is similar to the case of a grounded ferrite slab.¹ The good agreement between the $|S_{21}|$ and $|S_{12}|$ curves indicates the validity of the extraction approach. The rotation angle has a small

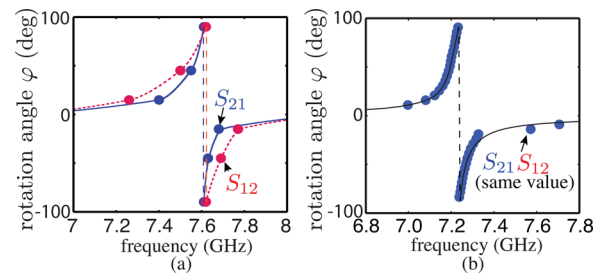


FIG. 8. (Color online) Polarization rotation angle φ versus frequency. (a) Experimental results. (b) Full-wave simulation results.

positive value for frequencies below 7 GHz, then it monotonically increases with frequency, up to the resonance frequency (7.61 GHz). At resonance, φ flips sign, exactly as in ferrites, and then increases towards 0 for frequencies beyond 8 GHz. The rotation angle has also been obtained through full-wave numerical simulations via the CST Microwave Studio (based on the finite integration technique), as shown in Fig. 8(b). The shape of the simulation curve is very close to the experimental one. The observed discrepancy in the resonance frequency, which is of about 0.4 GHz, is attributed to difference in the substrate permittivity and in the transistor S-parameters between measurements and simulations.

This work has been carried out under the sponsorship of the NSERC Strategic Project Grant No. 1014 and KAKENHI No. 23686054. The authors would like to acknowledge CST Corporation for their generous donation of software licenses.

¹B. Lax and K. J. Button, *Microwave Ferrites and Ferrimagnetics* (McGraw-Hill, New York, 1962).

²M. V. Freiser, *IEEE Trans. Magn.* **2**, 152 (1968).

³C. Caloz and T. Itoh, *Electromagnetic Metamaterials, Transmission Line Theory and Microwave Applications* (Wiley, New York, 2005).

⁴R. Marqués, F. Martín, and M. Sorolla, *Metamaterials with Negative Parameters: Theory, Design and Microwave Applications* (Wiley, New York, 2008).